Prepublished copy

Nature Environment & Pollution Technology

This is a peer-reviewed prepublished version of the paper

Original Research

Estimation of High-Resolution Surface Soil Moisture Through GIS-Based Frequency Ratio Modeling

Sailesh Samanta†

School of Surveying and Land Studies, The Papua New Guinea University of Technology, Lae, Morobe Province, Papua New Guinea

†Corresponding author: Sailesh Samanta; rsgis.sailesh@gmail.com

ORCID: https://orcid.org/0000-0002-0535-5535

Key Words	Frequency ratio, Geographic information system, High-resolution, Remote sensing, Markham River, Soil moisture
DOI	https://doi.org/10.46488/NEPT.2025.v24i04.D1775 (DOI will be active only after the final publication of the paper)
Citation for the Paper	Samanta, S., 2025. Estimation of high-resolution surface soil moisture through GIS-based frequency ratio modeling. *Nature Environment and Pollution Technology*, 24(4), p. D1775. https://doi.org/10.46488/NEPT.2025.v24i04.D1775

Abstract: This article presents a methodology for estimating higher-resolution soil moisture using GIS and frequency ratio (FR) modeling techniques. A global soil moisture database with a 9 km spatial resolution was used as reference data. A total of 283 reference points were selected through spatial fishnet analysis with optimum soil moisture. Eighty percent (80%) of these reference points served as inputs to the FR model, with the remaining twenty percent (20%) reserved for validation. Key independent variables incorporated in the FR modeling process included land use and land cover, soil characteristics, vegetation index, wetness index, surface temperature, rainfall, elevation, slope, and distance from rivers. This research was conducted in the final drainage basin of the Markham River basin. The resulting high-resolution surface soil moisture was further classified into five basic zones, namely very low (< 6), low (6 - 7), moderate (7 - 8), high (8 - 9), and very high (> 9). The result indicates almost 26.10% and 56.89% of the Basin area come under high and very high soil moisture zones respectively. The FR model evinced a prediction accuracy of 93.98% along with a succession rate of 91.59%. These results provide useful data for scientific applications in various domains, specifically in the agricultural sector, local government administrator, researcher, and planner.

1. INTRODUCTION

The availability of optimum soil moisture is necessary for optimal crop production, agriculture drought monitoring (Zhu et al. 2019), flood preparedness (Pegram et al. 2010), water supply management, and agricultural monitoring. The earlier report and research indicated that agriculture production consumed 70% of total freshwater (Pimentel et al. 2004; Connor 2015; Paquin and Cosgrove 2016) and it may increase to 90% by 2050 (Sophocleous 2004). The global agriculture industries are facing several challenges related to water resources, like water shortage, water surfeit, water pollution, unsustainable water use, etc. (Rosegrant et al. 2009). These conditions are being worsened by population growth, urbanization, climate change, and threatening food security (Srivastav et al. 2021). Management of water and policies for water supply as well as watershed management can reduce this effect. Soil moisture is one of the paramount factors that affect agriculture growth, health, and yield (Furtak and Wolińska 2023).

The presence of water on the upper surface of the soil is termed soil moisture (Svetlitchnyi et al. 2003), which is also affected by the evaporation or transpiration process (Lawrence et al. 2007). The presence of water within 10cm of the topsoil is called surface soil moisture and within 200 cm is called root zone soil moisture (Manfreda et al. 2014; Yinglan et al. 2022). Measuring soil moisture in rugged terrain can prove difficult using traditional field methods (Crow et al. 2012). In such cases, modern technology like geographic information systems (GIS) has increased importance for modeling and spatial mapping soil moisture (Mulder et al. 2011; Rani et al. 2022). Several comprehensive tools are available, which researchers use to assess or model soil moisture content. The traditional method, the Soil and water assessment tool (SWAT) estimates moisture content based on the standard rainfall index (Havrylenko et al. 2016). It is also useful to estimate the amount of stream flow (Wang et al. 2008). The soil conservation service curve number (SCS-CN) can estimate runoff based on soil and land use/land cover combination under a storm rainfall (Pal and Samanta 2011). The topography-based hydrological model (TOPMODEL) is another model used by many researchers to simulate soil moisture and runoff in watershed areas (Tombul 2007; Zhu et al. 2009; Fu et al. 2018). Another traditional model, the bridging event and continuous hydrological (BEACH) can predict the probability of soil moisture based on rainfall, soil type, topography, and crop pattern (Sheikh et al. 2009). Traditional models require in-situ data, including soil samples, rainfall measurements, river discharge, and topographic information to be collected from the ground. This process is very expensive and may not cover a large area. Furthermore, very few gauge stations are available in Papua New Guinea (Chua et al. 2023), which presents a drawback of working with traditional models. An alternative option is modern technology like remote sensing, which is cost-effective and can cover a vast area.

Presently, satellite remote sensing technologies have proven the reliability of soil moisture prediction. A strong relationship is found between the soil moisture content and land surface temperature (LST) (Cammalleri and Vogt 2015; Ghahremanloo et al. 2019). Research has been conducted based on machine learning algorithms to estimate soil moisture, where normalized difference

vegetation index (NDVI) and climate data are two major factors in alpine grassland (Wang and Fu 2023). Temperature vegetation dryness index (TVDI) derived from the combination of NDVI and LST has been used to estimate soil moisture (Sandholt et al. 2002; Park et al. 2014; Zhao et al. 2021). Recently several researches have been carried out to estimate moisture in 1 km spatial resolution (Zeng et al. 2015; Meng et al. 2019). The microwave-based soil moisture measurements are relatively coarse (3 to 9 km) (Entekhabi et al. 2010; Zhang et al. 2020; Nguyen et al. 2023). GIS is utilized to create maps of soil surface moisture derived from passive microwave data and to assess the spatial arrangement of soil moisture. A recent research effort analyzes soil moisture intensity by integrating GIS-generated depth-to-water (DTW) table maps with soil-type maps (Mohtashami et al. 2023). Several researchers confirmed that different models, tools, and algorithms estimate soil moisture, but it is not clear which method is the best (Nguyen et al. 2022; Tramblay and Segui 2022; Kisekka et al. 2022). Different statistical modeling approaches have been applied for the estimation, modeling, and spatial mapping of soil moisture and its spatial variation (Lookingbill and Urban 2004; Ahmad et al. 2010; Hosseini et al. 2015; Pal et al. 2016; Aires et al. 2021). Some recent studies focused on forecasting soil moisture at different time scales, namely the long short-term memory (LSTM) method. The technique works based on weights assigned based on physical knowledge (Li et al 2022). The prediction through LSTM was highly accurate for short-term frames compared to the long-term. To overcome the issue a multi-head LSTM model was introduced which enhances the prediction in hourly, daily, and monthly intervals based on multiple hypotheses and a weighted averaging method (Datta and Faroughi 2023).

Frequency ratio (FR) modeling is a statistical, quantitative, and probability approach for simulating the quality of the environment (Laaidi et al. 2003; Tehrany et al. 2018), flood hazard assessment (Samanta et al. 2018; Arabameri et al. 2019), landslide susceptibility mapping (Arabameri et al. 2019; Mersha and Meten 2020; Khan et al., 2024), groundwater potential mapping (Guru at al. 2017) based on topographical and environmental conditions. The FR model can demarcate a flood-prone area by analyzing the connection between flood events and flood factors, including elevation, slope, land use, distance from the river, and others. This model examines the correlation between landslides and various factors to develop landslide susceptibility maps. FR models also identify potential groundwater zones by analyzing groundwater occurrences and important factors, such as hydrogeomorphology, drainage density, geology, and more. FR model is a favorite method due to its easy application, simplicity, and relatively good prediction compared to other techniques, specifically when data sets are limited (Ozdemir and Altural 2013). FR model yielded the highest accuracy compared to the analytic hierarchy process (AHP) for landslide susceptibility assessment (Panchal and Shrivastava 2021). The prediction and succession rate curve are found to be very impressive compared to the statistical index (SI) and weights of evidence (WoE) (Razavizadeh et al. 2017). Several machine learning models, like logistics regression (LR), random forest (RF), support vector machines (SVM), and decision tree (DT) require large amounts of training data and are more complex to implement and

interpret than the FR model (Meng et al. 2024). The SWAT approach simulates water and sediment dynamics on a watershed scale based on complex calibration, which requires extensive data input and is not suitable for smaller and highly variable watersheds (Thokchom 2020) compared to the FR model. TOPMODEL is the topography-based hydrological model used to simulate watershed hydrology. TOPMODEL works based on numerous parameters and assumptions, which creates uncertainties (Jeziorska and Niedzielski 2018).

This research is an ensemble method, which used frequency ratio (FR) a statistical approach for estimating high-spatial resolution soil moisture (30 m) depending on several environmental and topographic parameters like land use land cover (LULC), NDVI, LST, topographic wetness index (TWI), topographic altitude, slope of the land, rainfall, soil texture, and proximity to the river. High spatial resolution (30m) soil moisture data are vital for precision agriculture, drought and flood monitoring and forecasting, and water resource management. The spatial variability of soil moisture across the landscape can be captured easily using high-resolution data sets compared to courser resolution data sets (9 km spatial resolution). The high-resolution data sets represent improved spatial variability and spatial accuracy compared to SMAP products (Vergopolan et al. 2021). This research aimed to estimate surface soil moisture zones in the final flow Basin of Markham River. The objectives of this study were to create wall-to-wall datasets on conditioning environmental and topographic factors into the FR model, create a higher spatial resolution (30 m) soil moisture zone database, and finally, validate the FR model based on prediction accuracy and succession rate.

2. STUDY LOCATION AND MATERIALS

The final flow basin in the lower basin of the Markham River which has a land area of 1806.85 square kilometers is selected as the research area. It is situated between longitudes 146.09º E and 174.04º E and latitudes 6.23º S and 6.78º S (Figure 1). The Finisterre range is the source the Markham River, which empties into the Huon Gulf (Renagi et al. 2010). The upper basin region spans approximately 12800 square kilometers and is characterized by steep slopes, rough terrain, thick forest, and drainage (Sam et al. 2020). The study area experiences hot and humid weather throughout the year (Ningal et al. 2008). In the research region, 4200 mm of total rainfall falls annually. Most of the basin's soils have a modest amount of drainage. The month of June through October is usually the dry season in this area (Prentice and Hope 2007). Because of the decreased rainfall, a progressive deterioration in soil moisture conditions was also observed. This has a significant impact on crop output; thus, farmers should think about moisture-saving management techniques.

Several microwave sensors are accruing global soil moisture data. The spatial resolution is very low, which is around 9 km. Soil Moisture Active Passive (SMAP) is a satellite mission designed to measure the presence or quantity of water in the topsoil of the Earth (Reichle et al. 2014). The onboard

radiometer (*L-band)* is designed to investigate moisture variability (Sales et al. 2007; Escorihuela et al. 2010). Algorithm Theoretical Basis Documents (ATBDs) are used to generate of SMAP database (Reichle et al. 2019; Chan et al. 2013). SMAP has two immediate parameters, namely global root zone soil moisture and global surface soil moisture (Reichle et al. 2012). The average of 3-hourly geophysical data of a particular day is estimated to be the 1200 - 1500 hours data sets. These data sets are freely available to use without restrictions for science and application users (Reichle et al. 2022a). The SMAP geospatial data set (for the date of 23rd September 2023: 1200 - 1500 hrs.) was downloaded from https://nsidc.org/ in h5 format (Reichle et al. 2022b) and further processed in ArcGIS v10.5 to re-format, re-project, and subset as per the study area. Advanced space-borne thermal emission and reflection radiometer (ASTER) provide an elevation model for the globe in 30 m spatial resolution (Abrams et al. 2020). Landsat 8 operational land imager (OLI) was freely downloaded from http://earthexplorer.usgs.gov. Furthermore, after the radiometric enhancement and rearrangement of the spectral bands, the image was clipped as per the study area for further use. Other GIS data layers, like soil texture and rainfall, were taken from the existing GIS database of the Papua New Guinea Resource Information System.

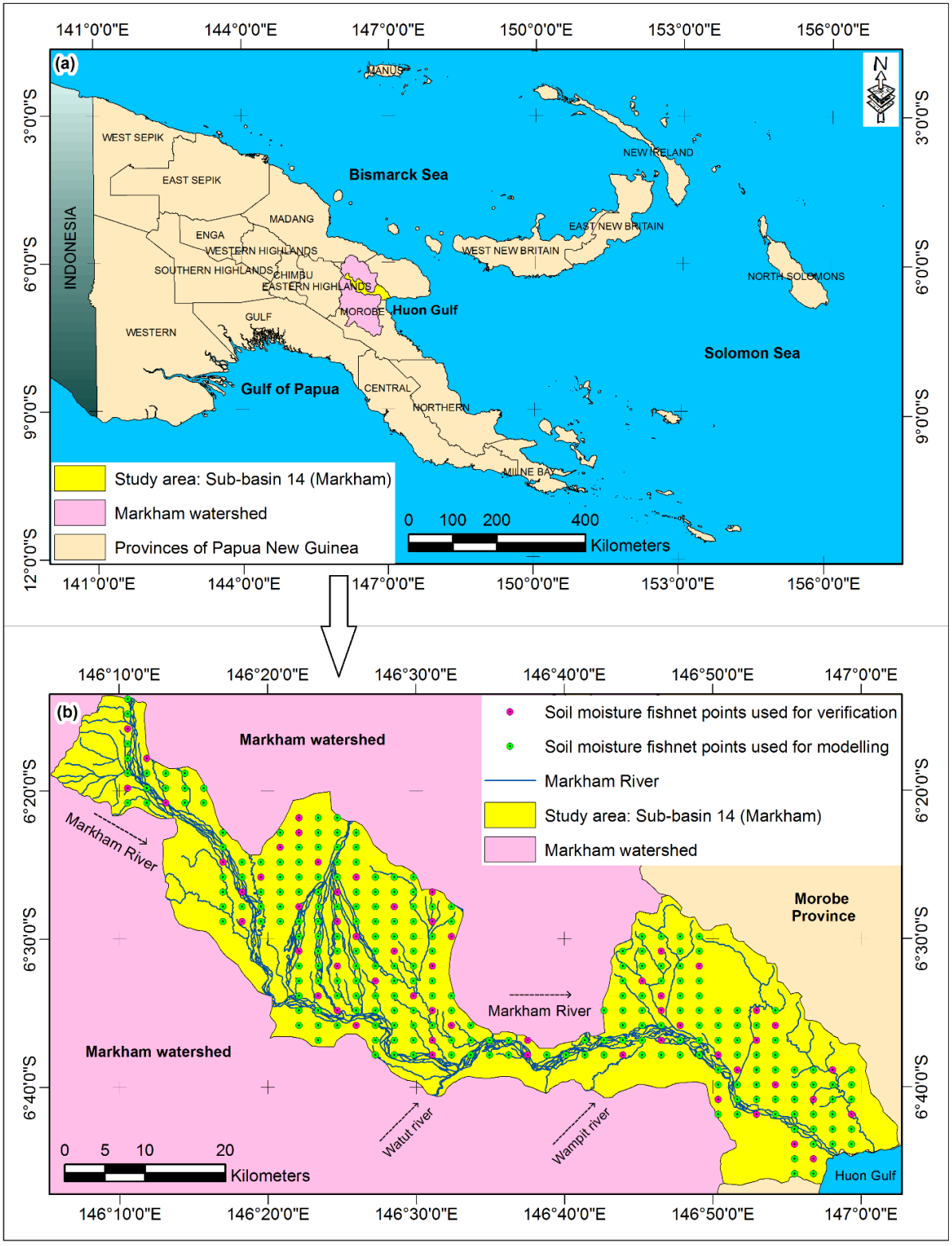

Fig. 1: Location map of the Study area (a) Papua New Guinea with the Markham watershed and (b) The study area sub-basin no.14.

3. METHODOLOGY

Estimation of soil moisture was carried out based on nine-fold (9) geospatial parameters based on the consultation of local soil scientists and agricultural experts. They are LULC, NDVI, soil texture, LST, TWI, rainfall, elevation, slope, and distance from the river. Geospatial layers were constructed from satellite remote sensing images and the national-level GIS database of PNG. After supervised classification, a LULC map was generated from the standard false colour bands of Landsat 8 satellite data. Soil texture map and rainfall map were developed from the national-level GIS database of PNG. A proximity analysis in ArcGIS v10.5 was performed to develop distance from the drainage network Elevation and slope were calculated from ASTER GDEM. TWI and LST data sets were generated from DEM and TIRS data through the topographic wetness model and surface temperature model respectively. TWI database was prepared based on the basin area length of contour and slope of the land in degrees as presented in equation 1 (Beven and Kirkby 1979; Samanta et al. 2018).

$$\text{TWI} = \text{Ln}\left(\frac{\text{a}}{\text{tanB}}\right) \quad \ldots(1)$$

TWI stands for the topographic wetness index, a refers to catchment further denoted as "A/L", A refers to the area of the basin and L is the length of a contour, B stands for the slope of the land.

Several analyses were performed to prepare the TWI database for the study area, namely (i) calculating the direction of the flow, (ii) generating flow accumulation, (iii) preparing the slope of the land in degree, (iv) creation of radian slope of the land, (v) calculation of tan slope, and finally (vi) scaled flow accumulation (Kopecký et al. 2021). Similarly, a series of calculations were performed to derive LST from TIRS bands, like (a) extraction of spectral radiance value, (b) calculation of brightness temperature, (c) calculation of NDVI, (d) generating proportion of vegetation database, (e) derivation of surface emissivity of the land, and finally (f) obtain the land surface temperature map (De Jesus et al. 2017; Wang et al. 2019).

SMAP dataset was used as a reference database for this study. The Frequency model requires adequate training events to calculate the frequency ratio value for each conditioning factor and their subclasses. A fishnet analysis was performed to create reference points with known soil moisture values. "Create fishnet" is a Geo-processing tool under the data management of Arc Toolbox within ArcGIS (Akter and Javed 2022). It can create a feature class in a net of rectangular cells based on user-provided information, such as the number of rows and columns. The resulting fishnet layer can be restricted with the spatial extent of the input study area extension. Each fishnet cell contains a point label at the center of each cell. These points were used to derive moisture value from the raster-based SMAP data through "extract value to point" analysis. SMAP provides soil moisture values between 1 and 0, which represents extreme wet to extreme dry conditions respectively (Saha et al. 2021). Furthermore, SM

values of more than 0.3 are considered optimum (no drought) conditions for plant growth (Parida et al. 2008). Initially total number of 412 reference points were created through spatial fishnet analysis for the study area. Further analysis was conducted to select reference points with optimum moisture levels and 283 reference points were selected with moisture levels of more than 0.35 and 0.30 at the root zone and surface soil respectively. A spatial query was performed to identify these reference points from the initial population. Eighty percent (80%) of these reference points (226) served as inputs to the FR model, with the remaining twenty percent (20%) point (57) reserved for the validation process (Bashir et al. 2023; Taffese and Espinosa-Leal 2023). The spatial resolution of all the data sets was not the same. To overcome this issue all the datasets were resampled to a common resolution (30m spatial resolution) using nearest-neighbor resampling techniques in the ArcGIS platform (Gurjar and Padmanabhan 2005).

FR method is a bivariate statistical analysis method for the simulation of environmental situations, which considers conditional factors as dependent variables. FR model calculates FR value which expresses the type of correlation between parameters and potential soil moisture. The calculation of the FR value was processed using equation 2, where E represents several reference points for each subclass, F represents the total reference point, M stands for the histogram of each subclass and L stands for the total histogram (Bonham-Carter 1994; Samanta et al. 2018). FR value represents the proportion of the ratio factor between several reference points for each subclass and the total reference point, as well as the ratio of each subclass' histogram to the total histogram. A higher value indicates a higher correlation and a lower refers to a weak between the conditioning factor and potential soil moisture respectively (Tehrany et al. 2014).

$$\mathrm{FR} = \frac{(E/F)}{(M/L)} \quad \ldots(2)$$

After the calculation of the FR value, the frequency ratio index (FRI) was calculated using Equation 3 (Samanta et al., 2018). The calculated FRI represents the soil moisture index (SMI) as shown in Equation 4. Higher value indicates higher moisture content or wet soil and lower refers to the lower moisture content or dry soil.

$$\mathrm{FRI} = \Sigma\,\mathrm{FR} \quad \ldots(3)$$

$$\mathrm{SMI} = \mathrm{FRI} \quad \ldots(4)$$

4. RESULTS AND DISCUSSION

Different conditioning factors play specific roles in estimating high-resolution surface soil moisture databases. Nine (9) conditioning factors were selected carefully for this research, namely LULC, NDVI, LST, TWI, soil texture, rainfall, elevation, slope, and distance from rivers. The spatial

distribution pattern of these parameters was mapped and statistical databases were built with their sub-classes (Figure 2 and Table 1). The classification produces a LULC database that presents a total of nine (9) major classes. They are dense Forest, low dense forest, shrub land, outcrop/barren land, mountain grassland, urban and built-up, inland water, river water, and agriculture. The low dense forest is the dominant class (35.38%) mostly spread over the eastern, western, and some pockets of the southern region (Figure 2a). Shrubland is the second largest land cover class (26%) dominated in the middle portion and some pockets of northern and eastern parts. A total FR index of 7.44 was contributed by LULC for the FR model. The highest frequency ratio (FR) value (1.41) was calculated for shrubland (Table 1) based on the FR equation (Equation 8), which indicates a higher correlation with the moisture level in the soil (Kidron and Gutschick 2013). As per the United States Department of Agriculture (USDA) classification scheme, nine (9) textural classes, namely (i) silty clay, (ii) silty clay loam, (iii) sandy loam, (iv) sandy clay loam, (v) silty loam, (vi) sand, (vii) sandy clay, (viii) loamy sand and (xi) clay are found in this research area (Figure 2b). Sandy clay loam is the largest soil texture class (31.57%) dominated in the middle portion, where the floodplain is located. The clay class (1.13%) is found in some pockets of the eastern part and contributes a maximum frequency ratio (FR) value of 1.57 as a single subclass. The maximum total FR index of 9.33 was contributed by the soil texture parameter into the FR model compared to other parameters (Table 1), which describes a robust correlation with the available moisture content in the soil (Petrone et al. 2004; Takada et al. 2009).

NDVI has a dynamic response to soil moisture variation (Ahmed et al. 2017). The output NDVI value ranges from -0.39 to 0.67 (Figure 2c) and categorised into five (5) different zones, namely (i) less than 0.1 (20.24 %), (ii) 0.1 - 0.15 (13.19 %), (iii) 1.15 - 0.30 (18.62 %), (iv) 0.30 - 0.45 (31.83 %), and (v) more than 0.45 (16.11 %). FR value of 1.41 is calculated for the 2nd category (0.1 – 0.15) and a total FR index of 5.20 is contributed by the soil texture parameter into the FR model (Table 1). There is a reverse relationship between LST and surface soil moisture except in higher latitude locations (Ghahremanloo et al. 2019; Jiang et al. 2023). The modeled LST of this area is varied from 9º to 47º centigrade (C) and further grouped into five (5) classes, namely (i) less than 20º C (3.03%), (ii) 20º C - 25º C (15.36 %), (iii) 25º C - 30º C (61.44 %), (iv) 30º C - 35º C (17.03%), and (v) more than 35º C (3.14 %). The highest temperature is observed in the township area in the eastern part and some pockets of middle and northwest parts of the research location (Figure 2d).

TWI quantifies the topography-based soil moisture variation (Raduła et al. 2018; Kopecký et al. 2021). The calculated TWI varied between 0.47 and 42.31 (Figure 2e). The maximum range of TWI is spread over the middle part of the watershed area where the topographic slope is very gentle (Qin et al., 2011). The spatial database of TWI was further reclassified into five (5) categories, namely (i) less than 5.0 (4.43 %), (ii) 5.0 – 7.5 (38.46 %), (iii) 7.5 – 10.0 (38.10 %), (iv) 10.0 – 12.5 (9.09 %), and (v) more than 12,.5 (9.91 %). LST and TWI contribute a total FR index of 4.76 and 4.87 to the FR model respectively (Table 1). Rainfall is the primary source of Soil moisture and also depends on the quantity

and continuity of the rainfall (Sehler et al. 2019). The average yearly rainfall recorded between 1350 mm and 3850 mm, which was categorised into five (5) different groups, specifically (i) less than 1500 mm (0.85 %), (ii) 1500 mm to 2000 mm (14.55 %), (iii) 72000 mm to 2500 mm (57.11 %), (iv) 2500 mm to 3000 mm (10.22 %), and (v) more than 3000 mm (17.27 %) (Figure 2f and Table 1).

Elevation and slope have a greater impact on surface soil moisture (Moeslund et al. 2013). As water flows downhill under the influence of gravity, the higher elevation areas are characterized by lower soil moisture and lower elevation areas are dominated by higher moisture conditions (Qiu et al. 2001; Cai et al., 2019). The elevation data was categorized into five (5) different groups, namely (i) less than 200 m (63.84 %), (ii) 200 m to 400 m (21.39 %), (iii) 400 m to 600 m (6.54 %), (iv) 600 m to 800 m (3.92 %), and (v) more than 800 m (4.82 %) (Figure 2g). The slope database was divided into five (5) categories. They are (i) less than 2º (53.59 %), (ii) 2º to 5º (14.55 %), (iii) 5º to 10º (7.87 %), (iv) 10º to 20º (13.43 %), and (v) more than 20º (10.55 %). A higher slope (More than 20º) is found in the mountain range located in the northeast, southeast, and northwest of the research area (Figure 2h). Both gentle slope (less than 2º) and lower altitude (less than 200 m) are found in the middle section of the basin. Elevation and slope parameters shared a total FR index of 3.27 and 4.16 in the FR model respectively (Table 1). In general, soil moisture varies by distance from the river (Horvath, 2002). Soil situated near the river is characterised by higher moisture than soils located at a distance from the river (Kumar et al., 2016). Five different buffer areas were generated through proximity analysis from the river, such as (i) less than 200 m (24.62 %), (ii) 200 m to 400 m (14.04 %), (iii) 400 m to 600 m (10.85 %), (iv) 600 m to 800 m (8.40 %), and (v) more than 800 m (42.09 %) (Table 1).

Table 1: Conditioning factors used for estimation of soil moisture (SM) through the FR model.

Value	Class name or Description	Histogram	% of Histogram	Potential SM points	% of Potential SM points	Frequency ratio (FR)	Total FR index
			LULC				
1	Dense Forest	47374	2.36	2	0.885	0.37	
2	Low dense forest	710143	35.38	68	30.088	0.85	
3	Shrub land	521832	26.00	83	36.726	1.41	
4	Outcrop/barren lands	43242	2.15	2	0.885	0.41	
5	Mountain grassland	421354	20.99	35	15.487	0.74	
6	Urban and built-up	15443	0.77	2	0.885	1.15	7.44
7	Inland water	4765	0.24	0	0.000	0.00	
8	River water	140449	7.00	19	8.407	1.20	
9	Agriculture	102468	5.11	15	6.637	1.30	
			Soil Texture				
1	Silty clay	91671	4.57	2	0.88	0.19	
2	Sandy loam	176212	8.78	19	8.41	0.96	

3	Sandy clay loam	633631	31.57	68	30.09	0.95	
4	Silty clay loam	406699	20.26	43	19.03	0.94	
5	Clay	22672	1.13	4	1.77	1.57	
6	Silty loam	22603	1.13	3	1.33	1.18	9.33
7	Sandy clay	14248	0.71	0	0.00	0.00	
8	Sand	555087	27.66	78	34.51	1.25	
10	Loamy sand	84247	4.20	9	3.98	0.95	
			NDVI				
1	Lower than 0.1	406280	20.24	47	20.80	1.03	
2	0.1 - 0.15	264815	13.19	42	18.58	1.41	
3	1.15 - 0.30	373813	18.62	38	16.81	0.90	
4	0.30 - 0.45	638820	31.83	63	27.88	0.88	5.20
5	Higher than 0.45	323342	16.11	36	15.93	0.99	
			LST in degree C				
1	Less than 20	60822	3.03	3	1.33	0.44	
2	20 - 25	308266	15.36	20	8.85	0.58	
3	25 - 30	1233168	61.44	149	65.93	1.07	4.76
4	30 - 35	341812	17.03	43	19.03	1.12	
5	More than 35	63002	3.14	11	4.87	1.55	
			TWI				
1	Less than 5.0	88958	4.43	6	2.65	0.60	
2	5.0 - 7.5	771982	38.46	76	33.63	0.87	4.87
3	7.5 - 10.0	764626	38.10	95	42.04	1.10	
4	10.0 - 12.5	182526	9.09	26	11.50	1.27	
5	More than 12.5	198978	9.91	23	10.18	1.03	
			Rainfall in mm				
1	Less than 1500	16990	0.85	2	0.88	1.05	
2	1500 - 2000	292094	14.55	25	11.06	0.76	
3	2000 - 2500	1146286	57.11	148	65.49	1.15	4.65
4	2500 - 3000	205126	10.22	22	9.73	0.95	
5	More than 3000	346574	17.27	29	12.83	0.74	
			Elevation in m				
1	Less than 200	1281891	63.87	162	71.68	1.12	
2	200 - 400	429324	21.39	50	22.12	1.03	
3	400 - 600	131360	6.54	10	4.42	0.68	3.27
4	600 - 800	78617	3.92	3	1.33	0.34	
5	More than 800	85878	4.28	1	0.44	0.10	
			Slope in degree				
1	Less than 2	1075600	53.59	144	63.72	1.19	
2	2 - 5	292084	14.55	39	17.26	1.19	
3	5 - 10	157971	7.87	11	4.87	0.62	4.16
4	10 - 20	269603	13.43	20	8.85	0.66	
5	More than 20	211812	10.55	12	5.31	0.50	
			Distance from the river in m				
1	Less than 200	494112	24.62	59	26.11	1.06	
2	200 - 400	281756	14.04	40	17.70	1.26	

3	400 - 600	217794	10.85	21	9.29	0.86	5.06
4	600 - 800	168666	8.40	18	7.96	0.95	
5	More than 800	844742	42.09	89	39.38	0.94	

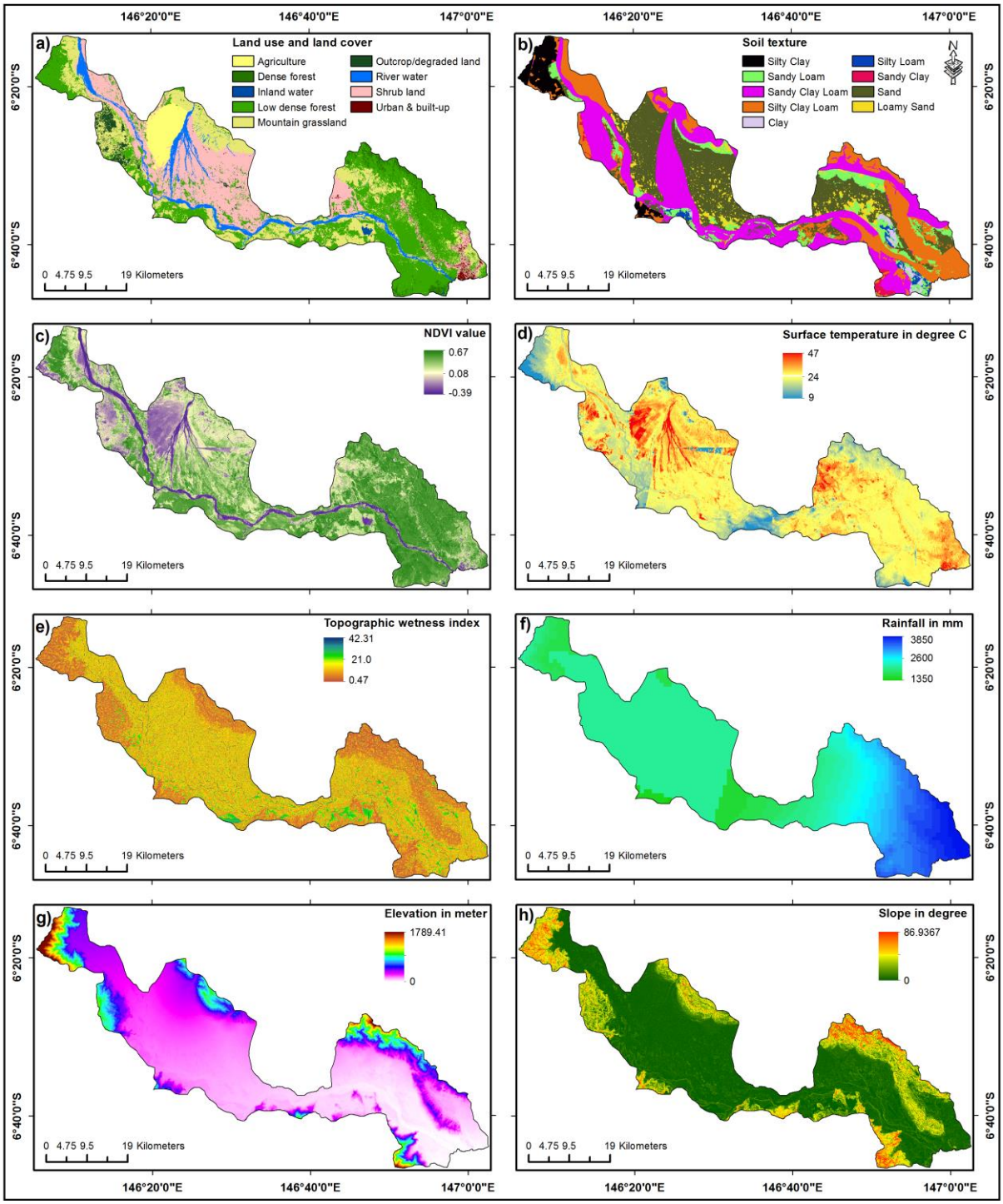

Fig. 2: Parameters used for FR modeling (a) LULC, (b) soil texture, (c) NDVI, (d) LST, (e) TWI, (f) rainfall, (g) elevation, and (h) slope characteristics of the study area.

The rating was assigned to each sub-class of all the nine conditioning parameters based on the FR value presented in Table 1. The FR value is ranged from 0 to 1.57. The total FR index was calculated for each parameter after aggregation of all FR values sponsored by individual sub-classes. Finally, the overlay analysis was performed after integrating all the parameters with their FR characteristics based on equation 3, and the high-resolution (30 m) SMI database was constructed. The resulting SMI ranged from 4.57 to 11.61 with an average index value of 9.01 (Figure 3a). A higher soil moisture index value indicates wet soil and a lower index indicates dry soil. The resulting soil moisture index database was further reclassified into five (5) soil groups based on surface soil moisture index. They are (i) very low moisture (less than 6.0), (ii) low moisture (6.0 to 7.0), (iii) moderate moisture (7.0 to 8.0), (iv) high moisture (8.0 to 9.0), and (v) very high moisture (More than 9.0) (Figure 2b). The result identifies that almost 56.89 % of the basin is termed as very high and 26.10 % as high moisture level (Table 2) and these relatively wet soil classes are identified within the floodplain area of the basin. These areas are enriched with higher moisture content because of higher topographic wetness index, lower elevation, and flat slopes (Figure 2). Shrubland, sandy clay loam, lower NDVI, moderate surface temperature, and proximity to the river are the other dominant characteristics that cause higher moisture levels in these areas.

Table 2: Different soil moisture zones based on classified SMI.

Class no.	Soil moisture class	FR index range	Histogram	% Area
1	Very low	Less than 6	42461	2.12
2	Low	6 - 7	94519	4.71
3	Moderate	7 - 8	204339	10.18
4	High	8 - 9	523870	26.10
5	Very high	More than 9	1141881	56.89

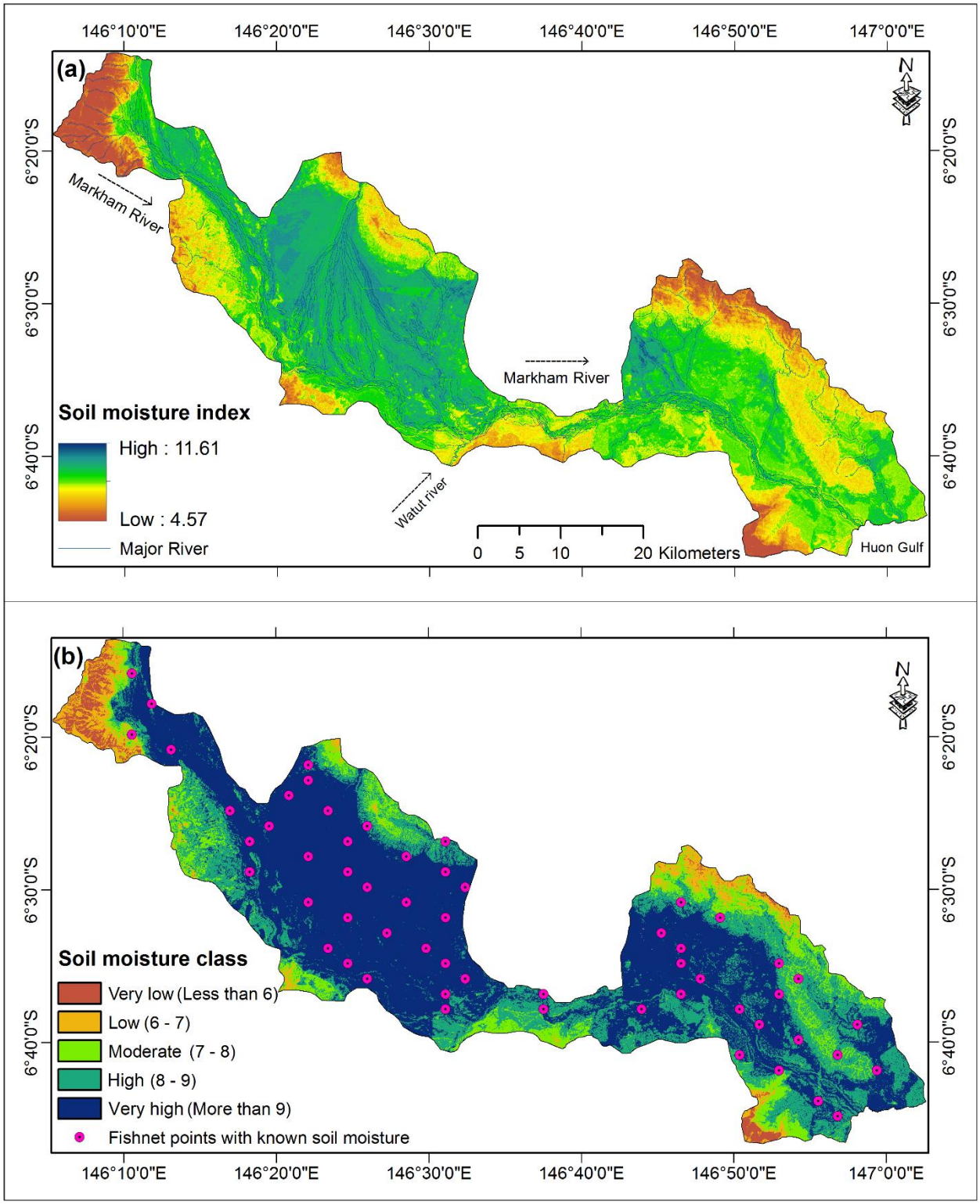

Fig. 3: Estimated SMI (a) Spatial distribution pattern of SMI (b) validation using 20% legacy soil moisture reference point.

Estimation of a high-resolution surface soil moisture database was generated in the final sub-basin of the Markham River basin through the FR statistical approach. Although the reference point

datasets were generated from 9 km SMAP level-4 data through fishnet analysis, the FR model generates a high-resolution database (30 meters). A statistical spatial interpolation process can forecast at unknown locations based on known information (Srivastava et al. 2019; Salahalden et al. 2024), but the critical or location variation can't be incorporated into the prediction. So, the FR model is an alternative statistical method was selected for this study (Snepvangers et al. 2003). The topographic slope, elevation, TWI, and LST were measured statistically using linear trend line analysis (R-squared) to determine how well they fit the regression model (Shaw et al. 2023). The coefficient of determination (R-squared) values for topographic slope, elevation, NDVI, TWI, and LST were calculated through linear regression analysis. TWI and soil moisture were found to have a moderate relationship, with a calculated coefficient of determination (R squared) of 0.29. Although soil properties have an impact, a strong correlation was found between slope and soil moisture (0.67). The relationship between elevation and soil moisture was determined to be 0.46. However, due to the complexity of the terrain, the correlation between NDVI and soil moisture is very low (0.19), while the correlation between NDVI and LST with soil moisture is moderate (0.27).

Resampling techniques enhance data compatibility and visualization, enabling all the data sets to be at a common resolution (30m spatial resolution). Additionally, they streamline the analysis procedure. However, depending on the resampled techniques employed, they introduce certain uncertainties, such as fine-scale data loss and distortion. In contrast to the bilinear and cubic approaches, the nearest neighbor method can maintain the original value in the unaltered datasets (Lyons et al. 2018). Accuracy and success rate are essential to validate model-based estimation of soil moisture (Delgoda et al. 2016; Chi et al. 2019). The resulting SMI database was validated through prediction accuracy and success rate. In landslide susceptibility mapping using the Frequency Ratio (FR) model, benchmarks for success rate and prediction accuracy typically range from 70% to 80%, with some studies showing success rates as high as 90% and prediction rates around 87% (Bhandari et al. 2024). The success rate was computed as 91.59% (Table 3) and the prediction accuracy of the estimation was calculated as 93.98% (Table 3), which is very good evidence to validate the FR model in the estimation of high-resolution SMI. The FR model has been proven to be the best option over the MCDA approach because the FR model estimates better efficiency compared to any GIS-based MCDA model (Khosravi 2016; Wang and Li 2017).

Table 3: Prediction accuracy and succession rate of the SMI estimation.

Moisture category	FR index range	Validation [20% flood points]	Accuracy (high and very high class)	Prediction Accuracy %)	Training [80% flood points]	Success ((high and very high class)	Success Rate (%)
Very low	Less than 6	0			0		
Low	6 - 7	1			2		
Moderate	7 - 8	3	53	93.98%	17	207	91.59%
High	8 - 9	13			38		

Very high	More than 9	40		169	
	Total	57		226	

5. CONCLUSION

The estimation of surface soil moisture was conducted at the spatial resolution of 30 m (pixel size) based on LULC, soil texture NDVI, LST, TWI, rainfall, elevation, slope, and distance from the river. The spatial resolution of all the input conditioning parameters was in 30-meter pixels. It was investigated that soil moisture index distribution depends mostly on the TWI, LST, slope, soil type, proximity to the river, and vegetation. Topographic slope, elevation, TWI, and LST are important independent parameters for soil moisture estimation in selected catchment areas. A total of 283 reference points were selected in a specified interval with known soil moisture conditions. Eighty percent of these reference points (226) were used as inputs and the remaining twenty percent (57) were kept to validate the FR model estimation. The prediction accuracy of 93.98% validates the FR model prediction as acceptable and realistic. Remote sensing, GIS, and FR models are promising in hydrological research. FR model produces results with better prediction efficiency compared to any other GIS-based MCDA model (Wang and Li 2017; Samanta et al. 2017; Zeleke 2019). These results provide useful data for scientific applications in various domains, specifically in the agricultural sector, local government administrator, researcher, and planner. Soil moisture databases are efficiently used for watershed characterization, water balance studies, soil respiration, hydrology, soil health monitoring, plant growth, plant water stress, and irrigation scheduling. The FR modeling can be incorporated into practical hydrological decision-making by examining the connections between events and conditioning factors, aiding in the reduction of hydrological hazards and regional development. It can evaluate the correlation between dependent variables, such as crop health and production, and independent variables like soil quality, irrigation practices, climate, and more.

This study was focused on the estimation of the high-resolution surface soil moisture data based on the Frequency Ratio model, where 80% of the data was used as training and 20% was used for validation. Further research is recommended to use other machine learning methods to compare the results of the FR model to find its robustness. The establishment of ground-based combined models over larger catchment areas is required to generate accurate and precise multi-temporal soil moisture on a daily, weekly, or monthly basis with high-resolution soil moisture databases.

Author Contributions: This research is done by one author

Funding: No funding was received to conduct this research

Data availability: Data is provided within the manuscript

Institutional Review Board Statement: Not applicable

Informed Consent Statement: Not applicable

Acknowledgments: The author is thankful to the School of Surveying and Land Studies, under the Faculty of Built Environment at the Papua New Guinea University of Technology for all the facilities to carry out this research.

Conflicts of Interest: The authors declare no conflicts of interest.

REFERENCES

1. Abrams, M., Crippen, R. and Fujisada, H., 2020. ASTER global digital elevation model (GDEM) and ASTER global water body dataset (ASTWBD). *Remote Sensing*, *12*(7), 1156. https://doi.org/10.3390/rs12071156.
2. Ahmad, S., Kalra, A. and Stephen, H., 2010. Estimating soil moisture using remote sensing data: A machine learning approach. *Advances in water resources*, *33*(1), pp.69-80. https://doi.org/10.1016/j.advwatres.2009.10.008.
3. Ahmed, M., Else, B., Eklundh, L., Ardö, J. and Seaquist, J., 2017. Dynamic response of NDVI to soil moisture variations during different hydrological regimes in the Sahel region. *International Journal of Remote Sensing*, *38*(19), pp.5408-5429. https://doi.org/10.1080/01431161.2017.1339920.
4. Aires, F., Weston, P., de Rosnay, P. and Fairbairn, D., 2021. Statistical approaches to assimilate ASCAT soil moisture information—I. Methodologies and first assessment. *Quarterly Journal of the Royal Meteorological Society*, *147*(736), pp.1823-1852. https://doi.org/10.1002/qj.3997.
5. Akter, S. and Javed, S. A., 2022. GIS-based assessment of landslide susceptibility and inventory mapping using different bivariate models. *Geocarto International*, *37*(26), pp.12913-12942. https://doi.org/10.1080/10106049.2022.2076907.
6. Arabameri, A., Pradhan, B., Rezaei, K. and Lee, C.W., 2019. Assessment of landslide susceptibility using statistical-and artificial intelligence-based FR–RF integrated model and multiresolution DEMs. *Remote Sensing*, *11*(9), 999. https://doi.org/10.3390/rs11090999.
7. Bashir, R.N., Bajwa, I.S., Iqbal, M.W., Ashraf, M.U., Alghamdi, A.M., Bahaddad, A.A., Almarhabi, K.A., 2023. Leaching Fraction (LF) of irrigation water for saline soils using machine learning. *Intelligent Automation & Soft Computing*, *36*, pp.1915-1930. https://doi.org/10.32604/iasc.2023.030844.
8. Beven, K.J. and Kirkby, M.J., 1979. A physically based, variable contributing area model of basin hydrology/Un modèle à base physique de zone d'appel variable de l'hydrologie du bassin

versant. *Hydrological sciences journal*, *24*(1), pp.43-69. https://doi.org/10.1080/02626667909491834.

9. Bhandari, B. P., Dhakal, S. and Tsou, C. Y., 2024. Assessing the prediction accuracy of frequency ratio, weight of evidence, Shannon entropy, and information value methods for landslide susceptibility in the Siwalik Hills of Nepal. *Sustainability*, *16*(5), 2092. https://doi.org/10.3390/su16052092.
10. Bonham-Carter, G.F., 1994. Geographic information systems for geoscientists-modeling with GIS (No. 13), Elsevier. ISBN 0080424201.
11. Cai, Y., Zheng, W., Zhang, X., Zhangzhong, L. and Xue, X., 2019. Research on soil moisture prediction model based on deep learning. *PloS one*, *14*(4), e0214508. https://doi.org/10.1016/j.jhydrol.2019.01.046.
12. Cammalleri, C. and Vogt, J., 2015. On the role of land surface temperature as proxy of soil moisture status for drought monitoring in Europe. *Remote sensing*, *7*(12), pp.16849-16864. https://doi.org/10.3390/rs71215857.
13. Chan, S., Bindlish, R., Hunt, R., Jackson, T. and Kimball, J., 2013. Vegetation water content. *Jet Propulsion Laboratory, California Institute of Technology: Pasadena, CA, USA*. https://smap.jpl.nasa.gov/files/smap2/047_veg_water.pdf
14. Chua, Z. W., Kuleshov, Y., Watkins, A. B., Choy, S. and Sun, C., 2023. A Statistical Interpolation of Satellite Data with Rain Gauge Data over Papua New Guinea. *Journal of Hydrometeorology*, *24*(12), pp.2369-2387. https://doi.org/10.1175/JHM-D-23-0035.1.
15. Connor, R., 2015. *The United Nations world water development report 2015: water for a sustainable world* (Vol. 1). UNESCO publishing. ISBN 9789231000713.
16. Crow, W.T., Berg, A.A., Cosh, M.H., Loew, A., Mohanty, B.P., Panciera, R., Rosnay, P.D., Ryu, D. and Walker, J.P., 2012. Upscaling sparse ground-based soil moisture observations for the validation of coarse-resolution satellite soil moisture products. *Reviews of Geophysics*, *50*(2), RG2002. https://doi.org/10.1029/2011RG000372.
17. De Jesus, J.B. and Santana, I.D., 2017. Estimation of land surface temperature in caatinga area using Landsat 8 data. *Journal of Hyperspectral Remote Sensing*, *7*(3), pp.150-157. https://periodicos.ufpe.br/revistas/jhrs/article/download/22766/pdf
18. Delgoda, D., Saleem, S.K., Malano, H. and Halgamuge, M.N., 2016. Root zone soil moisture prediction models based on system identification: Formulation of the theory and validation using field and AQUACROP data. *Agricultural Water Management*, *163*, pp.344-353. https://doi.org/10.1016/j.agwat.2015.08.011.
19. Entekhabi, D., Njoku, E.G., O'neill, P.E., Kellogg, K.H., Crow, W.T., Edelstein, W.N. et. al., 2010. The soil moisture active passive (SMAP) mission. *Proceedings of the IEEE*, *98*(5), pp.704-716. https://doi.org/10.1109/JPROC.2010.2043918.

20. Escorihuela, M.J., Chanzy, A., Wigneron, J.P. and Kerr, Y.H., 2010. Effective soil moisture sampling depth of L-band radiometry: A case study. *Remote Sensing of Environment*, *114*(5), pp.995-1001. https://doi.org/10.1016/j.rse.2009.12.011.
21. Fu, X., Luo, L., Pan, M., Yu, Z., Tang, Y. and Ding, Y., 2018. Evaluation of TOPMODEL-based land surface–atmosphere transfer scheme (TOPLATS) through a soil moisture simulation. *Earth Interactions*, *22*(15), pp.1-19. https://doi.org/10.1175/EI-D-17-0037.1.
22. Furtak, K. and Wolińska, A., 2023. The impact of extreme weather events as a consequence of climate change on the soil moisture and on the quality of the soil environment and agriculture–A review. *Catena*, *231*, 107378. https://doi.org/10.1016/j.catena.2023.107378.
23. Ghahremanloo, M., Mobasheri, M.R. and Amani, M., 2019. Soil moisture estimation using land surface temperature and soil temperature at 5 cm depth. *International journal of remote sensing*, *40*(1), pp.104-117. https://doi.org/10.1080/01431161.2018.1501167.
24. Gurjar, S. B. and Padmanabhan, N., 2005. Study of various resampling techniques for high-resolution remote sensing imagery. *Journal of the Indian Society of Remote Sensing*, *33*, pp.113-120. https://doi.org/10.1007/BF02989999.
25. Guru, B., Seshan, K. and Bera, S., 2017. Frequency ratio model for groundwater potential mapping and its sustainable management in cold desert, India. *Journal of King Saud University-Science*, *29*(3), pp.333-347. https://doi.org/10.1016/j.jksus.2016.08.003.
26. Havrylenko, S.B., Bodoque, J.M., Srinivasan, R., Zucarelli, G.V. and Mercuri, P., 2016. Assessment of the soil water content in the Pampas region using SWAT. *Catena*, *137*, pp.298-309. https://doi.org/10.1016/j.catena.2015.10.001.
27. Horváth, S., 2002. Spatial and temporal patterns of soil moisture variations in a sub-catchment of River Tisza. *Physics and Chemistry of the Earth*, Parts A/B/C, *27*(23-24), pp.1051-1062. https://doi.org/10.1016/S1474-7065(02)00141-9.
28. Hosseini, R., Newlands, N.K., Dean, C.B. and Takemura, A., 2015. Statistical modeling of soil moisture, integrating satellite remote-sensing (SAR) and ground-based data. *Remote Sensing*, *7*(3), pp.2752-2780. https://doi.org/10.3390/rs70302752.
29. Jiang, K., Pan, Z., Pan, F., Teuling, A.J., Han, G., An, P., Chen, X., Wang, L., Song, Y., Cheng, L., Zhang, Z., Huang, N., Ma, S., Gao, R., Zhang, Z., Men, J., Lv, X. and Dong, Z., 2023. Combined influence of soil moisture and atmospheric humidity on land surface temperature under different climatic background. *Iscience*, *26*(6), 106837. https://doi.org/10.1016/j.isci.2023.106837.
30. Jeziorska, J. and Niedzielski, T., 2018. Applicability of TOPMODEL in the mountainous catchments in the upper Nysa Kłodzka river basin (SW Poland). *Acta Geophysica*, *66*, pp.203-222. https://doi.org/10.1007/s11600-018-0121-6.
31. Khan, A., Khan, G., Minhas, M., Gardezi, S.H., Ahmed, J. and Abbas, N., 2024. Landslide Susceptibility Zonation Mapping Using Machine Learning Algorithms and Statistical Prediction at

Hunza Watershed Basin, Pakistan. *Nature Environment and Pollution Technology*, *23*(4), pp.1973-1993. https://doi.org/10.46488/NEPT.2024.v23i04.007.

32. Khosravi, K., Nohani, E., Maroufinia, E. and Pourghasemi, H.R., 2016. A GIS-based flood susceptibility assessment and its mapping in Iran: a comparison between frequency ratio and weights-of-evidence bivariate statistical models with multi-criteria decision-making technique. *Natural hazards*, *83*, pp.947-987. https://doi.org/10.1007/s11069-016-2357-2.
33. Kidron, G.J. and Gutschick, V.P., 2013. Soil moisture correlates with shrub–grass association in the Chihuahuan Desert. *Catena*, *107*, pp.71-79. https://doi.org/10.1016/j.catena.2013.02.001.
34. Kisekka, I., Peddinti, S.R., Kustas, W.P., McElrone, A.J., Bambach-Ortiz, N., McKee, L. and Bastiaanssen, W., 2022. Spatial–temporal modeling of root zone soil moisture dynamics in a vineyard using machine learning and remote sensing. *Irrigation science*, *40*(4), pp.761-777. https://doi.org/10.1007/s00271-022-00775-1.
35. Kopecký, M., Macek, M. and Wild, J., 2021. Topographic Wetness Index calculation guidelines based on measured soil moisture and plant species composition. *Science of the Total Environment*, *757*, 143785. https://doi.org/10.1016/j.scitotenv.2020.143785.
36. Kumar, M. T. and Rao, M. C., 2023. Studies on predicting soil moisture levels at Andhra Loyola College, India, using SARIMA and LSTM models. *Environmental Monitoring and Assessment*, *195*(12), 1426. https://doi.org/10.1007/s10661-023-12080-1.
37. Kumar, V., Sharma, A., Bhardwaj, R. and Thukral, A.K., 2016. Monitoring and characterization of soils from river bed of Beas, India, using multivariate and remote sensing techniques. *British Journal of Applied Science & Technology*, *12*(2), 1. *https://doi.org/10.9734/BJAST/2016/21611*.
38. Laaidi, M., Thibaudon, M. and Besancenot, J.P., 2003. Two statistical approaches to forecasting the start and duration of the pollen season of Ambrosia in the area of Lyon (France). *International Journal of Biometeorology*, *48*(2), pp.65-73. https://doi.org/10.1007/s00484-003-0182-2.
39. Lawrence, D.M., Thornton, P.E., Oleson, K.W. and Bonan, G.B., 2007. The partitioning of evapotranspiration into transpiration, soil evaporation, and canopy evaporation in a GCM: Impacts on land–atmosphere interaction. *Journal of Hydrometeorology*, *8*(4), pp.862-880. https://doi.org/10.1175/JHM596.1.
40. Li, Q., Zhu, Y., Shangguan, W., Wang, X., Li, L. and Yu, F., 2022. An attention-aware LSTM model for soil moisture and soil temperature prediction. *Geoderma*, *409*, 115651. https://doi.org/10.1016/j.geoderma.2021.115651.
41. Lookingbill, T. and Urban, D., 2004. An empirical approach towards improved spatial estimates of soil moisture for vegetation analysis. *Landscape Ecology*, *19*, pp.417-433. https://doi.org/10.1023/B:LAND.0000030451.29571.8b.
42. Lyons, M. B., Keith, D. A., Phinn, S. R., Mason, T. J. and Elith, J., 2018. A comparison of resampling methods for remote sensing classification and accuracy assessment. *Remote Sensing of Environment*, *208*, pp.145-153. https://doi.org/10.1016/j.rse.2018.02.026.

43. Maduako, I.N., Ndukwu, R.I., Ifeanyichukwu, C. and Igbokwe, O., 2017. Multi-index soil moisture estimation from satellite earth observations: comparative evaluation of the topographic wetness index (TWI), the temperature vegetation dryness index (TVDI) and the improved TVDI (iTVDI). *Journal of the Indian Society of Remote Sensing*, *45*, pp.631-642. https://doi.org/10.1007/s12524-016-0635-9.
44. Manfreda, S., Brocca, L., Moramarco, T., Melone, F. and Sheffield, J., 2014. A physically based approach for the estimation of root-zone soil moisture from surface measurements. *Hydrology and Earth System Sciences*, *18*(3), pp.1199-1212. https://doi.org/10.5194/hess-18-1199-2014.
45. Meng, X., Liu, X., Wang, Y., Zhang, H. and Guo, X., 2024. Submarine landslide susceptibility assessment integrating frequency ratio with supervised machine learning approach. *Applied Ocean Research*, *153*, 104237. https://doi.org/10.1016/j.apor.2024.104237.
46. Meng, X., Wang, H., Chen, J., Yang, M. and Pan, Z., 2019. High-resolution simulation and validation of soil moisture in the arid region of Northwest China. *Scientific reports*, *9*(1), 17227. https://doi.org/10.1038/s41598-019-52923-x.
47. Mersha, T. and Meten, M., 2020. GIS-based landslide susceptibility mapping and assessment using bivariate statistical methods in Simada area, northwestern Ethiopia. *Geoenvironmental disasters*, *7*, 20. https://doi.org/10.1186/s40677-020-00155-x.
48. Moeslund, J.E., Arge, L., Bøcher, P.K., Dalgaard, T., Odgaard, M.V., Nygaard, B. and Svenning, J.C., 2013. Topographically controlled soil moisture is the primary driver of local vegetation patterns across a lowland region. *Ecosphere*, *4*(7), 91. https://doi.org/10.1890/ES13-00134.1.
49. Mohtashami, S., Hansson, L. and Eliasson, L., 2023. Estimating Soil Strength Using GIS-Based Maps-A case study in Sweden. *European Journal of Forest Engineering*, *9*(2), pp.70-79. https://doi.org/10.33904/ejfe.1321075.
50. Mulder, V.L., De Bruin, S., Schaepman, M.E. and Mayr, T.R., 2011. The use of remote sensing in soil and terrain mapping—A review. *Geoderma*, *162*(1-2), pp.1-19. https://doi.org/10.1016/j.geoderma.2010.12.018.
51. Nguyen, T.M., Walker, J.P., Ye, N. and Kodikara, J., 2023. Toward an Improved Surface Roughness Parameterization Model for Soil Moisture Retrieval in Road Construction. *IEEE Transactions on Geoscience and Remote Sensing*, *61*, pp.1-13. https://doi.org/10.1109/TGRS.2023.3238367.
52. Nguyen, T.T., Ngo, H.H., Guo, W., Chang, S.W., Nguyen, D.D., Nguyen, C.T., Zhang, J., Liang, X.T.B. and Hoang, N.B., 2022. A low-cost approach for soil moisture prediction using multi-sensor data and machine learning algorithm. *Science of the Total Environment*, *833*, 155066. https://doi.org/10.1016/j.scitotenv.2022.155066.
53. Ningal, T., Hartemink, A.E. and Bregt, A.K., 2008. Land use change and population growth in the Morobe Province of Papua New Guinea between 1975 and 2000. *Journal of environmental management*, *87*(1), pp.117-124. https://doi.org/10.1016/j.jenvman.2007.01.006.

54. Ozdemir, A. and Altural, T., 2013. A comparative study of frequency ratio, weights of evidence and logistic regression methods for landslide susceptibility mapping: Sultan Mountains, SW Turkey. *Journal of Asian Earth Sciences*, *64*, pp.180-197. https://doi.org/10.1016/j.jseaes.2012.12.014.
55. Pal, B. and Samanta, S., 2011. Surface runoff estimation and mapping using remote sensing and geographic information system. *International Journal of Advanced Science and Technology*, *3*(2), pp.106-114. https://www.academia.edu/download/47075709/Surface_runoff_estimation_and_mapping_us20160707-6667-ugfw20.pdf
56. Pal, M., Maity, R. and Dey, S., 2016. Statistical modelling of vertical soil moisture profile: coupling of memory and forcing. *Water resources management*, *30*(6), pp.1973-1986. https://doi.org/10.1007/s11269-016-1263-4.
57. Panchal, S. and Shrivastava, A. K., 2021. A comparative study of frequency ratio, Shannon's entropy and analytic hierarchy process (AHP) models for landslide susceptibility assessment. *ISPRS International Journal of Geo-Information*, *10*(9), 603. https://doi.org/10.3390/ijgi10090603.
58. Paquin, M. and Cosgrove, C., 2016. *The United Nations world water development report 2016: water and jobs*. UNESCO for UN-Water. https://www.unwater.org/publications/un-world-water-development-report-2016.
59. Parida, B.R., Collado, W.B., Borah, R., Hazarika, M.K. and Samarakoon, L., 2008. Detecting drought-prone areas of rice agriculture using a MODIS-derived soil moisture index. *GIScience & Remote Sensing*, *45*(1), pp.109-129. https://doi.org/10.2747/1548-1603.45.1.109.
60. Park, J.Y., Ahn, S.R., Hwang, S.J., Jang, C.H., Park, G A. and Kim, S.J., 2014. Evaluation of MODIS NDVI and LST for indicating soil moisture of forest areas based on SWAT modeling. *Paddy and water environment*, *12*, pp.77-88. https://doi.org/10.1007/s10333-014-0425-3.
61. Pegram, G.G.S., Sinclair, S., Vischel, T. and Nxumalo, N., 2010. Soil moisture from satellites: Daily maps over RSA for flash flood forecasting, drought monitoring, catchment management & agriculture. *Water Research Commission Report*, (1683/1), 10. https://www.wrc.org.za/wp-content/uploads/mdocs/1683-1-101.pdf
62. Petrone, R.M., Price, J.S., Carey, S.K. and Waddington, J.M., 2004. Statistical characterization of the spatial variability of soil moisture in a cutover peatland. *Hydrological processes*, *18*(1), pp.41-52. https://doi.org/10.1002/hyp.1309.
63. Pimentel, D., Berger, B., Filiberto, D., Newton, M., Wolfe, B., Karabinakis, E., Clark, S., Poon, E., Abbett, E. and Nandagopal, S., 2004. Water resources: agricultural and environmental issues. *BioScience*, *54*(10), pp.909-918. https://doi.org/10.1641/0006-3568(2004)054[0909:WRAAEI]2.0.CO;2.
64. Prentice, M.L. and Hope, G.S., 2007. Climate of Papua. *The ecology of Papua*, *1*, pp.479-494. https://wwfint.awsassets.panda.org/downloads/prentice_hope_climate_papua_2006.pdf

65. Qin, C.Z., Zhu, A.X., Pei, T., Li, B.L., Scholten, T., Behrens, T. and Zhou, C.H., 2011. An approach to computing topographic wetness index based on maximum downslope gradient. *Precision agriculture*, *12*, pp.32-43. https://doi.org/10.1007/s11119-009-9152-y
66. Qiu, Y., Fu, B., Wang, J. and Chen, L., 2001. Soil moisture variation in relation to topography and land use in a hillslope catchment of the Loess Plateau, China. *Journal of Hydrology*, *240*(3-4), pp.243-263. https://doi.org/10.1016/S0022-1694(00)00362-0.
67. Raduła, M.W., Szymura, T.H. and Szymura, M., 2018. Topographic wetness index explains soil moisture better than bioindication with Ellenberg's indicator values. *Ecological indicators*, *85*, pp.172-179. https://doi.org/10.1016/j.ecolind.2017.10.011.
68. Rani, A., Kumar, N., Kumar, J. and Sinha, N.K., 2022. Machine learning for soil moisture assessment. In *Deep learning for sustainable agriculture*. Academic Press, pp.143-168. https://doi.org/10.1016/B978-0-323-85214-2.00001-X.
69. Razavizadeh, S., Solaimani, K., Massironi, M. and Kavian, A., 2017. Mapping landslide susceptibility with frequency ratio, statistical index, and weights of evidence models: a case study in northern Iran. *Environmental Earth Sciences*, *76*, pp.1-16. https://doi.org/10.1007/s12665-017-6839-7.
70. Reichle, R. H., Liu, Q., Koster, R. D., Crow, W. T., De Lannoy, G. J., Kimball, J. S., Ardizzone, J.V., Bosch, D., Colliander, A., Cosh, M. and Walker, J. P. (2019). Version 4 of the SMAP level-4 soil moisture algorithm and data product. *Journal of Advances in Modeling Earth Systems*, *11*(10), pp.3106-3130. https://doi.org/10.1029/2019MS001729.
71. Reichle, R., Crow, W., Koster, R., Kimball, J. and De Lannoy, G., 2012. SMAP level 4 surface and root zone soil moisture (L4_SM) data product. *Algorithm Theoretical Basis Doc*. https://asf.alaska.edu/wp-content/uploads/2019/03/l4_sm_initrel_v1_9.pdf
72. Reichle, R., Koster, R., De Lannoy, G., Crow, W. and Kimball, J., 2014. SMAP Algorithm Theoretical Basis Document: Level 4 Surface and Root Zone Soil Moisture (L4_SM) Data Product. SMAP Project, JPL D-66483, Jet Propulsion Laboratory, Pasadena, CA, USA. https://nsidc.org/sites/default/files/272_l4_sm_reva_web_0.pdf
73. Reichle, R.H., De Lannoy, G., Koster, R.D., Crow, W.T., Kimball, J.S., Liu, Q. and Bechtold, M., 2022a. *SMAP L4 Global 3-hourly 9 km EASE-Grid Surface and Root Zone Soil Moisture Geophysical Data, Version 7*. [Indicate subset used]. Boulder, Colorado USA. NASA National Snow and Ice Data Center Distributed Active Archive Center. https://doi.org/10.5067/EVKPQZ4AFC4D.
74. Reichle, R.H., De Lannoy, G., Koster, R.D., Crow, W.T., Kimball, J.S., Liu, Q. and Bechtold, M., 2022b. *SMAP L4 Global 3-hourly 9 km EASE-Grid Surface and Root Zone Soil Moisture Analysis Update, Version 7*. [Indicate subset used]. Boulder, Colorado USA. NASA National Snow and Ice Data Center Distributed Active Archive Center. https://doi.org/10.5067/LWJ6TF5SZRG3.

75. Renagi, O., Ridd, P. and Stieglitz, T., 2010. Quantifying the suspended sediment discharge to the ocean from the Markham River, Papua New Guinea. *Continental Shelf Research*, 30(9), pp.1030-1041. https://doi.org/10.1016/j.csr.2010.01.015.
76. Rosegrant, M. W., Ringler, C. and Zhu, T., 2009. Water for agriculture: maintaining food security under growing scarcity. *Annual review of Environment and resources*, *34*(1), pp.205-222. https://doi.org/10.1146/annurev.environ.030308.090351.
77. Saha, T.R., Shrestha, P.K., Rakovec, O., Thober, S. and Samaniego, L., 2021. A drought monitoring tool for South Asia. *Environmental Research Letters*, *16*(5), 054014. https://doi.org/10.1088/1748-9326/abf525.
78. Salahalden, V.F., Shareef, M.A. and Al Nuaimy, Q.A.M., 2024. Assessment of Deposited Red Clay Soil in Kirkuk City Using Remote Sensing Data and GIS Techniques. *Nature Environment & Pollution Technology*, *23*(2). https://doi.org/10.46488/NEPT.2024.v23i02.001
79. Saleh, K., Wigneron, J.P., Waldteufel, P., de Rosnay, P., Schwank, M., Calvet, J.C. and Kerr, Y.H., 2007. Estimates of surface soil moisture under grass covers using L-band radiometry. *Remote Sensing of Environment*, *109*(1), pp.42-53. https://doi.org/10.1016/j.rse.2006.12.002
80. Sam, N., Nimiago, P., McIntosh, P. and Wang, N., 2020. Markham river floodplain sediments reveal last glacial maximum erosion in Papua New Guinea uplands followed by landscape stability. *Quaternary Australasia*, *37*(1), pp.19-20. https://search.informit.org/doi/10.3316/informit.285736632870949
81. Samanta, S., Pal, D.K. and Palsamanta, B., 2018. Flood susceptibility analysis through remote sensing, GIS and frequency ratio model. *Applied Water Science*, *8*(2), 66. https://doi.org/10.1007/s13201-018-0710-1.
82. Sandholt, I., Rasmussen, K. and Andersen, J., 2002. A simple interpretation of the surface temperature/vegetation index space for assessment of surface moisture status. *Remote Sensing of environment*, *79*(2-3), pp.213-224. https://doi.org/10.1016/S0034-4257(01)00274-7.
83. Sehler, R., Li, J., Reager, J.T. and Ye, H., 2019. Investigating relationship between soil moisture and precipitation globally using remote sensing observations. *Journal of Contemporary Water Research & Education*, *168*(1), pp.106-118. https://doi.org/10.1111/j.1936-704X.2019.03324.x.
84. Shaw, M., Rights, J.D., Sterba, S.S. and Flake, J.K., 2023. r2mlm: An R package calculating R-squared measures for multilevel models. *Behavior Research Methods*, 55(4), pp.1942-1964. https://doi.org/10.3758/s13428-022-01841-4.
85. Sheikh, V., Visser, S. and Stroosnijder, L., 2009. A simple model to predict soil moisture: Bridging Event and Continuous Hydrological (BEACH) modelling. *Environmental Modelling & Software*, *24*(4), pp.542-556. https://doi.org/10.1016/j.envsoft.2008.10.005.
86. Snepvangers, J.J.J.C., Heuvelink, G.B.M. and Huisman, J.A., 2003. Soil water content interpolation using spatio-temporal kriging with external drift. *Geoderma*, *112*(3-4), pp.253-271. https://doi.org/10.1016/S0016-7061(02)00310-5.

87. Sophocleous, M. (2004). Global and regional water availability and demand: prospects for the future. *Natural Resources Research, 13,* pp.61-75. https://doi.org/10.1023/B:NARR.0000032644.16734.f5.
88. Srivastav, A. L., Dhyani, R., Ranjan, M., Madhav, S. and Sillanpää, M., 2021. Climate-resilient strategies for sustainable management of water resources and agriculture. *Environmental Science and Pollution Research*, *28*(31), pp.41576-41595. https://doi.org/10.1007/s11356-021-14332-4.
89. Srivastava, P.K., Pandey, P.C., Petropoulos, G.P., Kourgialas, N.N., Pandey, V. and Singh, U., 2019. GIS and remote sensing aided information for soil moisture estimation: A comparative study of interpolation techniques. *Resources*, *8*(2), 70. https://doi.org/10.3390/resources8020070.
90. Svetlitchnyi, A.A., Plotnitskiy, S.V. and Stepovaya, O.Y., 2003. Spatial distribution of soil moisture content within catchments and its modelling on the basis of topographic data. *Journal of Hydrology*, *277*(1-2), pp.50-60. https://doi.org/10.1016/S0022-1694(03)00083-0.
91. Taffese, W.Z., Espinosa-Leal, L., 2023. Multitarget regression models for predicting compressive strength and chloride resistance of concrete. *Journal of Building Engineering*, *72*, 106523. https://doi.org/10.1016/j.jobe.2023.106523.
92. Takada, M., Mishima, Y. and Natsume, S., 2009. Estimation of surface soil properties in peatland using ALOS/PALSAR. *Landscape and Ecological Engineering*, *5,* pp.45-58. https://doi.org/10.1007/s11355-008-0061-4.
93. Tehrany, M.S., Kumar, L., Jebur, M.N. and Shabani, F., 2018. Evaluating the application of the statistical index method in flood susceptibility mapping and its comparison with frequency ratio and logistic regression methods. *Geomatics, Natural Hazards and Risk*, *10*(1), pp.79-101. https://doi.org/10.1080/19475705.2018.1506509.
94. Tehrany, M.S., Lee, M.J., Pradhan, B., Jebur, M.N. and Lee, S., 2014. Flood susceptibility mapping using integrated bivariate and multivariate statistical models. *Environmental earth sciences*, *72*, pp.4001-4015. https://doi.org/10.1007/s12665-014-3289-3.
95. Thokchom, B., 2020. Water-related problem with special reference to global climate change in India. In *Water Conservation and Wastewater Treatment in BRICS Nations, Chapter 3,* pp.37-60. Elsevier. https://doi.org/10.1016/B978-0-12-818339-7.00003-5.
96. Tombul, M., 2007. Mapping field surface soil moisture for hydrological modeling. *Water resources management*, *21*, pp.1865-1880. https://doi.org/10.1007/s11269-006-9134-z.
97. Tramblay, Y. and Seguí, P.Q., 2022. Estimating soil moisture conditions for drought monitoring with random forests and a simple soil moisture accounting scheme. *Natural Hazards and Earth System Sciences*, *22*, pp.1325-1334. https://doi.org/10.5194/nhess-22-1325-2022.
98. Vergopolan, N., Chaney, N. W., Pan, M., Sheffield, J., Beck, H. E., Ferguson, C. R., Torres-Rojas, L., Sadri, S. and Wood, E. F., 2021. SMAP-HydroBlocks, a 30-m satellite-based soil moisture dataset for the conterminous US. *Scientific data*, *8*(1), 264. https://doi.org/10.1038/s41597-021-01050-2.

99. Wang, L., Lu, Y. and Yao, Y., 2019. Comparison of three algorithms for the retrieval of land surface temperature from Landsat 8 images. *Sensors*, *19*(22), 5049. https://doi.org/10.3390/s19225049.
100. Wang, S. and Fu, G., 2023. Modelling soil moisture using climate data and normalized difference vegetation index based on nine algorithms in alpine grasslands. *Frontiers in Environmental Science*, 11, 1130448. https://doi.org/10.3389/fenvs.2023.1130448.
101. Wang, X., Shang, S., Yang, W. and Melesse, A.M. 2008. Simulation of an agricultural watershed using an improved curve number method in SWAT. *Transactions of the ASABE*, *51*(4), pp.1323-1339. https://doi.org/10.13031/2013.25248.
102. Yinglan, A., Wang, G., Hu, P., Lai, X., Xue, B. and Fang, Q., 2022. Root-zone soil moisture estimation based on remote sensing data and deep learning. *Environmental Research*, *212*, 113278. https://doi.org/10.1016/j.envres.2022.113278
103. Zeleke, W.M. (2019). Wildfire Hazard Mapping using GIS-MCDA and Frequency Ratio Models: A Case Study in Eight Counties of Norway. Retrieved from https://urn.kb.se/resolve?urn=urn:nbn:se:hig:diva-31369.
104. Zeng, J., Li, Z., Chen, Q., Bi, H., Qiu, J. and Zou, P., 2015. Evaluation of remotely sensed and reanalysis soil moisture products over the Tibetan Plateau using in-situ observations. *Remote Sensing of environment*, *163*, pp.91-110. https://doi.org/10.1016/j.rse.2015.03.008.
105. Zhang, L., Meng, Q., Hu, D., Zhang, Y., Yao, S. and Chen, X., 2020. Comparison of different soil dielectric models for microwave soil moisture retrievals. *International Journal of Remote Sensing*, *41*(8), pp.3054-3069. https://doi.org/10.1080/01431161.2019.1698077.
106. Zhao, H., Li, Y., Chen, X., Wang, H., Yao, N. and Liu, F., 2021. Monitoring monthly soil moisture conditions in China with temperature vegetation dryness indexes based on an enhanced vegetation index and normalized difference vegetation index. *Theoretical and Applied Climatology*, *143*, pp.159-176. https://doi.org/10.1007/s00704-020-03422-x.
107. Zhu, Q., Luo, Y., Xu, Y.P., Tian, Y. and Yang, T., 2019. Satellite soil moisture for agricultural drought monitoring: Assessment of SMAP-derived soil water deficit index in Xiang River Basin, China. *Remote Sensing*, *11*(3), 362. https://doi.org/10.3390/rs11030362.
108. Zhu, X., Peng, W., Xu, J. and Yang, Y., 2009. Simulating the soil moisture and runoff in Baohe catchment based on TOPMODEL and DEM. In *2009 Third International Symposium on Intelligent Information Technology Application Workshops*, IEEE, pp.297-300. https://doi.org/10.1109/IITAW.2009.52.